URTeC: 2444366

Using Depletion-Zone Microseismicity to Understand Producing Volumes

Jonathan P. McKenna*, Michael H. Grealy, Michael S. Blaz and Nathan M. Toohey, MicroSeismic, Inc.

Summary

Studies have shown that proppant injected into fractures during hydraulic stimulation rapidly increases in packing density as fluids leak off into surrounding rock. Stresses are amplified at proppant grain contacts elevating the potential for stress-corrosion cracking and chemical potential at the contacts. Together, these effects promote immediate mechanical compaction and drive chemical compaction throughout engineering time scales (Lee et al, 2010). Draining the reservoir further enhances stresses leaving the reservoir critically-stressed as fractures close. Injection of fluid induces microseismicity that generally propagates away from injection ports as fluid induces fractures at rates that can be modeled using a pressure-diffusion model (Shapiro, 2009). When the front encounters a depleted reservoir on offset wells, pressures accelerate through the fluid-filled pore network inducing shear failure causing microseisms with observed apparent propagation velocities much higher than typical fracture propagation rates and can be used to delineate depleted fractures (Dohmen, 2013) forming a snapshot of production in time.

Microseismic data were collected during the treatment of a four-well pad in the Williston Basin. After five months of producing hydrocarbons from the first pad, a second pad was also treated and monitored proximal to the first. Microseismic events recorded during the second pad treatment extended toward and accelerated across the first pad, with the majority of offset activity occurring on the well closest to the second pad. By combining hypocenter locations, seismic moments, focal mechanisms, fluid leakoff, treatment volumes, and rock properties, we created a calibrated proppant-filled Discrete Fracture Network (DFN) model for each pad. To further condition the model for the second pad, we extended the methods of Shapiro and Dohmen to define multiple pressure-diffusion fronts to classify events associated with injected fluid, the offset pad, and depleted portions of the reservoir and utilized only fluid related events.

Microseismic event locations monitored during the second pad coincide with the modeled proppant-filled fractures derived from the treatment of the first pad. Furthermore, events consistent with Dohmen's depletion zone coincide with distal producing wells over 6000 ft. away from injection ports. Results suggest that offset well microseismicity is associated with the more conductive offset proppant-pack and can be used to quantify the actual proppant distribution, validate the propped DFN model and identify compacted portions of the depleted reservoir.

Method

Microseismic data was collected while fracturing two, four-well pads targeting both the Three Forks and Middle Bakken Formations (see Figure 2B). During stimulation of the second pad, microseismicity extended across the offset pad of wells that was previously treated. The data set was selected because a 1000 ft gap of untreated reservoir existed between the two pads which allowed unrestricted microseismic growth in between the pads, yielding insight into the propagation rate of the microseismicity associated with both the stimulated wells and the previously fractured offset wells. Additionally each stage of both pads was treated similarly, allowing for simple data aggregation.

Event Classification

Event classification was performed to identify different populations of events that might yield insight into the hydraulic-fracturing process and its impact on surrounding rock. Since we were interested in the rate that activity occurred after initially pressuring up each stage and since all stages were treated in a similar fashion, the primary variables analyzed were elapsed time into the treatment (t), distance from the center of the treated interval (r) and size/quality of the events (Signal to Noise Ratio (SNR)). Figure 1shows a plot of all three variables for all stages of the stimulated pad.

Treatment of each stage of the four wells were similar (slickwater volume followed by cross-linked fluid followed by 20/40 mesh sized proppant with cross-linked gel hitting formation at about 50 minutes into treatment). Therefore, we aggregated all stage data together to look for trends that might occur due to the same changes made during the stage treatment.

Fluid-induced events can be identified using Shapiro's method. Events were initially classified using an unsupervised hierarchical clustering methodology using a Ward's algorithm. In an attempt to define pressure diffusion fronts, attributes analyzed were pumping time, event distance from stage center and energy-semblance. The first two attributes are traditionally used to define the pressure diffusion front and backfront (Shapiro, 1997) and energy-semblance was added as an attribute in an attempt to classify different populations with Gaussian energy distributions. Figure 1 shows the classified events in r-t space with events sized by signal to noise ratio (SNR). Initially, the overall population shows a trend in the data forming during the early portion of the treatments (Figure 1, t<25 and r<700). However, the steepness of this trend abruptly increases at t>25; this is the point we hypothesize the microseismic event trend associated with the fluid, intersects the proppant pack of the offset well, thereby accelerating its propagation. If we continue the early trend through the bulk of the data, we see that the clustering algorithm also delineates a separation between groups of classified populations along the same trend. Slickwater was initially injected as the stimulation fluid, so we originated our curve to the beginning of slickwater injection at time t=0 and constrained the rest of the curve by following the separation discovered by the clustering. In this way, we can identify the pressure-diffusion front of the slickwater portion of the treatment (Figure 1 blue curve). Events above this curve are classified as "offset well", and below, "fluid".

Above the fluid-induced pressure diffusion front, the upper yellow population is a non-continuous population separated from the bulk of the offset well event population. This upper yellow population contains events with apparent velocities up to 50 times faster than the average velocity from the fluid-induced event population. We sub-divide the offset well population into 2 groups by initiating a curve at the point where the apparent velocity increases and constraining it by excluding the yellow population (Figure 1 orange curve). Events above this curve are classified as "depletion", or stress-induced events in drained portions of the reservoir.

Similarly, below the fluid-induced pressure diffusion front in Figure 1 (blue curve) the lower yellow population seems to be disconnected from the bulk of the main fluid-induced event population. During treatment of the wells, very viscous proppant-laden cross-linked gel was injected after the slickwater potion of the treatment and hits the formation on average at about 50 minutes into the treatment. We attempt to capture the events associated with the cross-linked gel by drawing a curve that encapsulates the lower yellow events and has an origin time of 50 minutes (Figure 1, yellow curve).

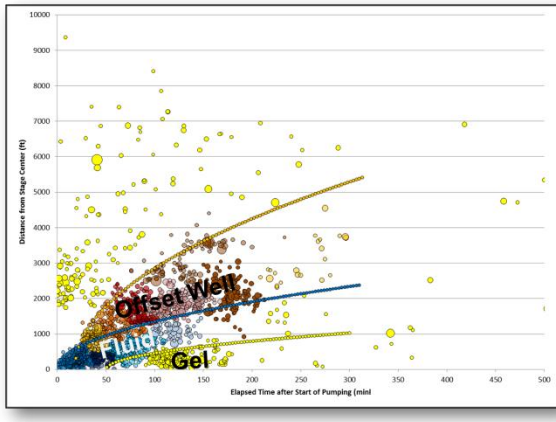

Figure 1: Map of microseismicity sized by signal to noise ratio (*SNR*) showing classification of events using Ward's algorithm. X-axis is elapsed time after start of pumping (*t*) and Y-axis is distance from stage center (*r*).

Figures 2A and 2B show a simplified classification of the events bounded by the previously defined pressure-diffusion fronts. The colors on both figures are consistent. Events associated with gel are yellow, slickwater fluid are blue, offset wells are orange, and events occurring on offset wells where depletion of the reservoir was occurring are black.

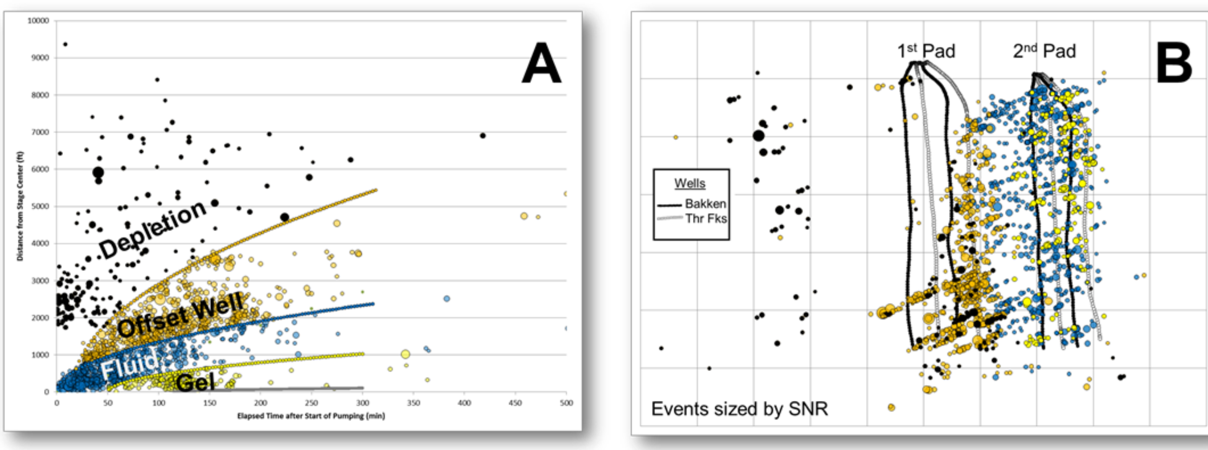

Figure 2: A - Plot of microseismicity sized by signal to noise ratio (SNR) showing classification of events associated with slickwater (Fluid, blue), the more viscous gel (Gel, yellow), events occurring on offset wells (Offset Well, orange), and events occurring on depleted wells (Depletion, black). B – Map showing locations of events shown in A using the same color scheme.

Modeling

A calibrated proppant-filled Discrete Fracture Network (DFN) model was created using a technique described by McKenna et al. (2015) to calculate fracture plane length, area and aperture based on the seismic moment of the fluid-induced microseismic events and associated shear modulus at each hypocenter location using a volumetric balance approach where the total fracture volume is equal to the injected slurry volume minus the volume due to leakoff into the formation. Fracture orientations are defined by the focal mechanism of the microseismic event. Proppant is injected into the DFN through the perforations of each stage and is filled outwards from the perforation location in an elliptical fashion that is informed by the stages shape of the microseismic cloud. We use the modeled results to yield insight into the actual proppant distributions which can help us understand what the offset well microseismicity is telling us.

Results

The modeled propped DFN (Figure 3A, green fractures) was created using the microseismicity detected during the original stimulation of the 1st pad (microseismicity from this pad is not shown). Figure 3B shows the perpendicular to wellbore distribution of the modeled propped DFN about their respective wellbores in black as well as the perpendicular to wellbore distribution of microseismic events about the easternmost Three Forks wellbore from the 1st pad (Figure 3B, outlined in white).

Visually, the green modeled propped fracture distribution on the easternmost well of the 1st pad (Figure 3A, dashed white circled well) coincides very well with the events that occurred on the easternmost offset well while treating the 2nd pad (Figure 3A, orange wells). By referencing the offset classified events to the offset well, the perpendicular (Figure 3B) and vertical (Figure 3C) distance to wellbore distributions of modeled propped fractures matches very closely with the distribution of the offset well population of microseismic events (Figure 3A dashed white circle). Both Figures 3B and 3C show that the distributions have peaks in the same locations, very similar distributions, and skewness in the same directions (westward for Figure 3B and upward for Figure 3C).

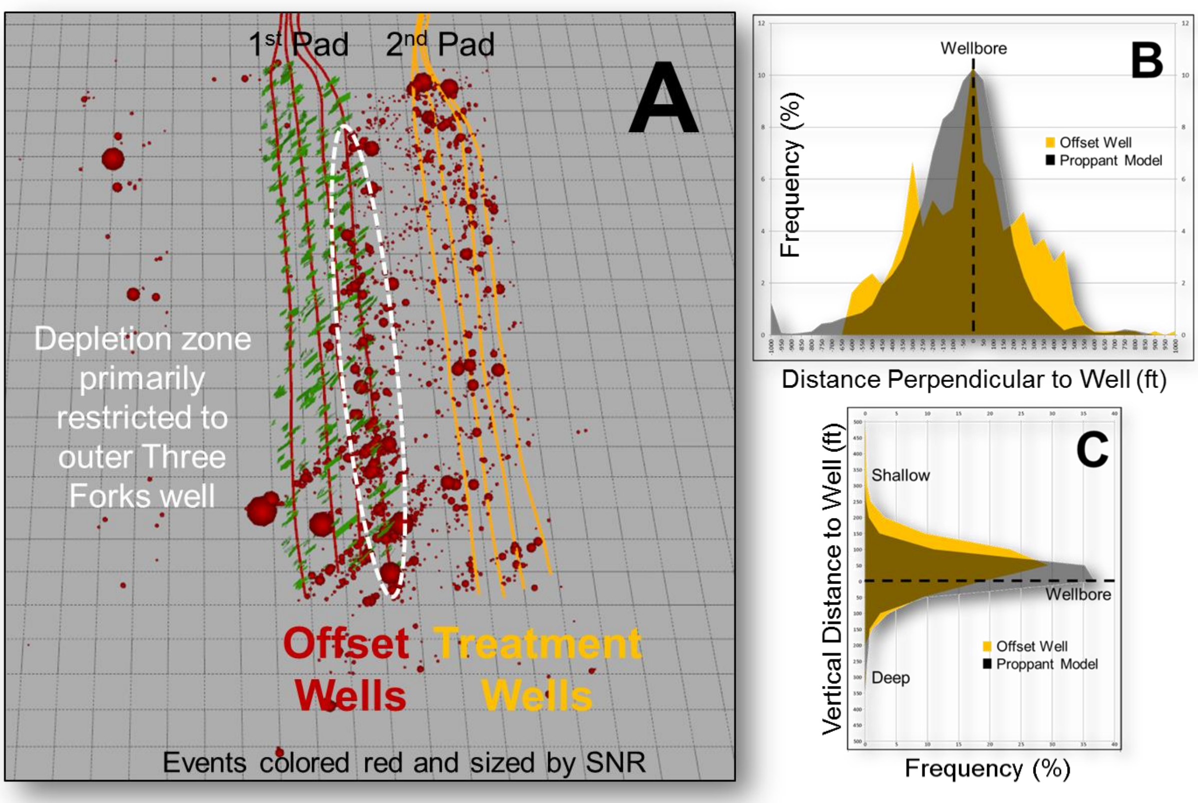

Figure 3: A – Map of microseismicity that occurred during the treatment of the 2nd pad (orange wells) and green modeled proppant-filled fractures using microseismicity from the treatment of the 1st pad (red wells). B – Perpendicular to wellbore distribution of modeled propped fractures (black) of the green fractures shown in A and distribution of offset well events (orange) shown in Figures 2A and 2B about the easternmost offset well (dashed white circled well in map view). C – Vertical distance to wellbore distribution of green propped fractures (black) and offset well events (orange) about the circled well shown in A.

Conclusions

By combining Dohmen's method for identifying microseismic events associated with regions of the depleted portions of the reservoir with Shapiro's method for identifying pressure-diffusion fronts associated with injected fluids, we have separated microseismic events associated with the fluids involved in stimulation from microseismic events that occurred on offset wells due to the depletion of the reservoir. Since the population of events on the offset wells coincides well with the modeled propped fractures in terms of perpendicular and vertical distribution about the wellbore, we conclude that the offset well activity is likely due to compaction of the proppant pack as fractures are closing due to decreased pore-pressures from draining the reservoir. If the pore throats of the offset well were already filled with incompressible fluid prior as the fluid front approached the offset-well proppant pack, a break-pedal type effect could initiate failure throughout the continuous depleted portion of the proppant pack. In addition, the match of the proppant distributions with the offset well distributions shown in Figures 3B and 3C also give validation to the modeled propped DFN methodology.

References

Dohmen, T., Zhang, J., Li, C., Blangy, J. P., Simon, K. M., Valleau, D. N., Ewles, J. D., Morton, S., and Checkles, S., 2013. A new surveillance method for delineation of depletion using microseismic and its application to development of unconventional reservoirs: Presented at SPE Annual Technical Conference and Exhibition, SPE 166274.

Lee, D.S., Elsworth, D., Yasuhara, H., Weaver, J.D., Rickman, R., 2010. Experiment and modeling to evaluate the effects of proppant-pack diagenesis on fracture treatments. J. Pet. Sci. Eng. 74 (1–2), 67–76.

McKenna, J.P., Quezada, O., Toohey, N.M, and Grealy, M.H., 2015. A data-driven proppant-filled fracture model: Comparing sliding sleeve and plug and perforation completion styles. Society of Exploration Geophysicists National Conference, New Orleans, LA.

Shapiro, S. A., and Dinske, C., 2009. Fluid-induced seismicity: Pressure diffusion and hydraulic fracturing, Geophys. Prospect. 57, no. 2007, 301–310, doi:10.1111/j.1365-2478.2008.00770.x.